J. Phys. B: At. Mol. Opt. Phys. **46** (2013) 035201 (5pp) doi:10.1088/0953-4075/46/3/035201

Single and double photoionization of Be and Mg

M S Pindzola[1], C P Ballance[1], Sh A Abdel-Naby[1], F Robicheaux[1], G S J Armstrong[2] and J Colgan[2]

[1] Department of Physics, Auburn University, Auburn, AL 36849, USA
[2] Theoretical Division, Los Alamos National Laboratory, Los Alamos, NM 87545, USA

Received 20 November 2012, in final form 18 December 2012
Published 16 January 2013
Online at stacks.iop.org/JPhysB/46/035201

Abstract
A new version of the time-dependent close-coupling method is used to calculate the single and double photoionization of the Be and Mg atoms. Total cross sections are calculated using an implicit time propagator with a core orthogonalization method on a variable radial mesh. The double to single photoionization cross section ratios are found to be in good agreement with experiment for both Be and Mg.

(Some figures may appear in colour only in the online journal)

1. Introduction

The double photoionization of atoms yields the emission of two free electrons moving in the field of a doubly charged atomic ion. Near the double ionization threshold the two slow moving free electrons interact strongly with each other and the residual ion core; a simple example of the quantal three-body Coulomb breakup problem. Experimental studies of the He atom have yielded double to single photoionization total cross section ratios [1], as well as double photoionization energy and differential cross sections [2]. In general, various non-perturbative theoretical approaches, including *R*-matrix methods [3–7], the converged close-coupling (CCC) method [8], the time-dependent close-coupling (TDCC) method [9], and the exterior complex scaling method [10], have yielded double photoionization cross sections in good agreement with experiment.

In recent years, both experiment and theory have studied the double photoionization of the alkaline-earth atoms. As one moves to heavier alkaline-earth atoms the double ionization threshold is lowered and the residual doubly charged atomic ion is no longer a point source. For the double photoionization of Be, theoretical calculations based on the CCC method [11], the TDCC method [12], and *R*-matrix methods [13, 14] are in good agreement with experiment [15, 16]. For the double photoionization of Mg, theoretical calculations based on the CCC method [17] and the *R*-matrix with pseudo-states (RMPS) method [14] are also in good agreement with experiment [18]. Non-perturbative calculations for the double photoionization of Ca have also been made using the hyperspherical *R*-matrix [19] and CCC [17] methods.

The TDCC method, based on an explicit time propagator with a core pseudopotential method on a fixed radial mesh, produces a range of cross sections for the double photoionization of Be that are in good agreement with measurements and other theoretical approaches. Total double photoionization cross sections are in reasonable agreement with synchrotron measurements [15, 16], while the energy and angle differential cross sections agree well with convergent close-coupling [11] and exterior complex-scaling [20] calculations. The core pseudopotential employed in the TDCC calculations smoothly removed the inner node from the 2s wavefunctions to avoid unphysical de-excitation to the inner 1s subshell. This approximation appears to work well, presumably because the inner node of the 2s orbital is close to the nucleus, and modifying the 2s orbitals in this portion of radial space does not seriously affect the photoionization process.

On the other hand, we have found that the explicit time propagator with a core pseudopotential approach applied to the double photoionization of Mg (and heavier systems) does not appear to work satisfactorily. In the Mg case, one must modify the 3s and 3p orbitals to avoid unphysical de-excitation. In particular, one must remove two nodes from the 3s orbital. The cross sections that result from this procedure are not in particularly good agreement with other approaches, and the double to single ionization ratio does not agree well with the measured value [18]. Attempts to use alternative forms of the pseudopotential [21] do not improve the comparison

with other work. Thus in this paper, we apply a new version of the TDCC method to calculate the double photoionization of the Be and Mg atoms. Our new version is based on an implicit time propagator with a core orthogonalization method on a variable radial mesh. The key step in the approach is the orthogonalization at each time step to the physical inner atomic orbitals to avoid the unphysical de-excitation of the active electrons as the time propagation proceeds. This is the first application of such a technique to the TDCC approach to atomic ionization. We find that the new version yields single and double photoionization cross sections that are in good agreement with experimentally measured ratios for both Be [16] and Mg [18].

The remainder of the paper is organized as follows: in section 2 we compare and contrast the explicit and implicit time propagators, as well as the core pseudopotential and core orthogonalization methods; in section 3 we present double to single photoionization cross section ratios in comparison with experiment; and in section 4 we conclude with a brief summary. Unless otherwise stated we will use atomic units.

2. Theory

The TDCC method [22] has been used to calculate the double photoionization cross sections for several light atoms. The six dimensional wavefunction for the two ionized electrons is expanded in coupled spherical harmonics and substituted into the time-dependent Schrödinger equation in the weak field limit to yield a set of (l_1, l_2) close-coupled equations given by

$$\begin{aligned} \mathrm{i}\frac{\partial P^{LS}_{l_1l_2}(r_1,r_2,t)}{\partial t} &= [T_{l_1}(r_1)+T_{l_2}(r_2)]P^{LS}_{l_1l_2}(r_1,r_2,t) \\ &+\sum_{l_1',l_2'} V^{L}_{l_1l_2,l_1'l_2'}(r_1,r_2)P^{LS}_{l_1'l_2'}(r_1,r_2,t) \\ &+\sum_{l_1',l_2'} W^{LL_0}_{l_1l_2,l_1'l_2'}(r_1,r_2,t)\bar{P}^{L_0S}_{l_1'l_2'}(r_1,r_2)\,\mathrm{e}^{-\mathrm{i}E_0t}\,, \end{aligned} \tag{1}$$

where

$$T_l(r) = -\frac{1}{2}\frac{\partial^2}{\partial r^2} + \frac{l(l+1)}{2r^2} - \frac{Z}{r} + U_l(r)\,, \tag{2}$$

Z is the nuclear charge, $U_l(r)$ is an atomic core potential, $V^{L}_{l_1l_2,l_1'l_2'}(r_1,r_2)$ is a two electron interaction operator, and $W^{LL_0}_{l_1l_2,l_1'l_2'}(r_1,r_2,t)$ is a time-dependent radiation field operator for the $L_0S \rightarrow LS$ transition. The correlated initial state radial wavefunctions, $\bar{P}^{L_0S}_{l_1l_2}(r_1,r_2)$, and energy, E_0, are obtained by relaxation of the time-dependent close-coupled equations in imaginary time given by

$$\begin{aligned} -\frac{\partial P^{L_0S}_{l_1l_2}(r_1,r_2,\tau)}{\partial \tau} &= [T_{l_1}(r_1)+T_{l_2}(r_2)]P^{L_0S}_{l_1l_2}(r_1,r_2,\tau) \\ &+\sum_{l_1',l_2'} V^{L_0}_{l_1l_2,l_1'l_2'}(r_1,r_2)P^{L_0S}_{l_1'l_2'}(r_1,r_2,\tau)\,, \end{aligned} \tag{3}$$

where $\bar{P}^{L_0S}_{l_1l_2}(r_1,r_2) = P^{L_0S}_{l_1l_2}(r_1,r_2,\tau\rightarrow\infty)$.

The initial condition for the solution of the close-coupled equations found in equation (1) is given by

$$P^{LS}_{l_1l_2}(r_1,r_2,t=0) = 0\,. \tag{4}$$

The solution of the close-coupled equations at later times may be obtained by using an explicit propagator:

$$\begin{aligned} P^{LS}_{l_1l_2}(r_1,r_2,t+\Delta t) &= P^{LS}_{l_1l_2}(r_1,r_2,t-\Delta t) \\ &-2\mathrm{i}\Delta t\Big([T_{l_1}(r_1)+T_{l_2}(r_2)]P^{LS}_{l_1l_2}(r_1,r_2,t) \\ &+\sum_{l_1',l_2'} V^{L}_{l_1l_2,l_1'l_2'}(r_1,r_2)P^{LS}_{l_1'l_2'}(r_1,r_2,t) \\ &+\sum_{l_1',l_2'} W^{LL_0}_{l_1l_2,l_1'l_2'}(r_1,r_2,t)\bar{P}^{L_0S}_{l_1'l_2'}(r_1,r_2)\,\mathrm{e}^{-\mathrm{i}E_0t}\Big). \end{aligned} \tag{5}$$

The solution of the close-coupled equations at later times may also be obtained by using an implicit propagator:

$$\begin{aligned} P^{LS}_{l_1l_2}(r_1,r_2,t+\Delta t) &= \sum_{l_1',l_2'}\exp\Big(-\mathrm{i}\frac{\Delta t}{2}V^{L}_{l_1l_2,l_1'l_2'}(r_1,r_2)\Big) \\ &\times\Big(1+\mathrm{i}\frac{\Delta t}{2}T_{l_1'}(r_1)\Big)^{-1} \\ &\times\Big(1+\mathrm{i}\frac{\Delta t}{2}T_{l_2'}(r_2)\Big)^{-1} \\ &\times\Big(1-\mathrm{i}\frac{\Delta t}{2}T_{l_2'}(r_2)\Big)\Big(1-\mathrm{i}\frac{\Delta t}{2}T_{l_1'}(r_1)\Big) \\ &\times\sum_{l_1'',l_2''}\exp\Big(-\mathrm{i}\frac{\Delta t}{2}V^{L}_{l_1'l_2',l_1''l_2''}(r_1,r_2)\Big)P^{LS}_{l_1''l_2''}(r_1,r_2,t) \\ &-\mathrm{i}\Delta t\sum_{l_1',l_2'} W^{LL_0}_{l_1l_2,l_1'l_2'}(r_1,r_2,t)\bar{P}^{L_0S}_{l_1'l_2'}(r_1,r_2)\,\mathrm{e}^{-\mathrm{i}E_0t}. \end{aligned} \tag{6}$$

The form of the implicit propagator found in equation (6) is similar to that used in the TDCC method for the electron-impact ionization of H_2^+ [23]. The key to accurate time propagation is that the $T_l(r)$ operator contains kinetic, nuclear, and atomic core terms. As the radial mesh spacing Δr becomes smaller, the time step Δt in the explicit method becomes quite small, while the time step Δt in the implicit method remains roughly constant. We also note for l_1l_2 coupled channels involving high angular momenta that the time step Δt in the explicit method becomes smaller, while in the implicit method it remains fairly constant.

The atomic core potential for the singly ionized atomic system is given by

$$U_l(r) = V_H(r) - \frac{\alpha_l}{2}\left(\frac{24\rho(r)}{\pi}\right)^{1/3}, \tag{7}$$

where $V_H(r)$ is the direct Hartree potential and $\rho(r)$ is the probability density in the local exchange potential. The bound radial orbitals needed to construct the atomic core potential are calculated using a Hartree–Fock atomic structure code [24] for the double ionized atomic system. The bound $P_{nl}(r)$ and continuum $P_{kl}(r)$ radial orbitals for the singly ionized atomic system are obtained by diagonalization of $T_l(r)$ of equation (2) on the radial lattice. The parameter α_l is varied to obtain accurate energy values for the first excited state for each l.

The problem of the unphysical de-excitation of either of the two active electrons to closed subshells during the time relaxation or propagation of the TDCC equations may be solved in either of two ways. The first way involves the use of a standard pseudopotential method. For example, for the double photoionization of the ground state of Mg, the inner nodes of the 3s and 3p orbitals may be smoothly removed and pseudopotentials $U_{PP0}(r)$ and $U_{PP1}(r)$ constructed by inverting the one electron radial Schrödinger equation. The one electron operators in the TDCC equations are now given by

$$T_l(r) = -\frac{1}{2}\frac{\partial^2}{\partial r^2} + U_{PPl}(r), \tag{8}$$

for $l = 0$ and $l = 1$, with equation (2) still used for $l \geqslant 2$. The second way involves the use of equation (2) for all l and a standard core-orthogonalization method for the inner subshells. For example, for the double photoionization of the ground state of Mg, the $P^{10}_{01}(r_1, r_2, t)$ radial wavefunction is orthogonalized at each time step Δt of the TDCC propagation of the ^{1}P excited state according to

$$\begin{aligned} P^{10}_{01}(r_1, r_2, t) &= P^{10}_{01}(r_1, r_2, t) \\ &- P_{1s}(r_1) \int dr'_1 P_{1s}(r'_1) P^{10}_{01}(r'_1, r_2, t) \\ &- P_{2s}(r_1) \int dr'_1 P_{2s}(r'_1) P^{10}_{01}(r'_1, r_2, t) \\ &- P_{2p}(r_2) \int dr'_2 P_{2p}(r'_2) P^{10}_{01}(r_1, r'_2, t) \\ &+ P_{1s}(r_1) P_{2p}(r_2) \\ &\times \int dr'_1 \int dr'_2 P_{1s}(r'_1) P_{2p}(r'_2) P^{10}_{01}(r'_1, r'_2, t) \\ &+ P_{2s}(r_1) P_{2p}(r_2) \\ &\times \int dr'_1 \int dr'_2 P_{2s}(r'_1) P_{2p}(r'_2) P^{10}_{01}(r'_1, r'_2, t) \, . \end{aligned} \tag{9}$$

Similar expressions are easily found for the $P^{00}_{00}(r_1, r_2, \tau)$ and $P^{00}_{11}(r_1, r_2, \tau)$ radial wavefunctions used in the TDCC relaxation of the ^{1}S ground state and the $P^{10}_{10}(r_1, r_2, t)$, $P^{10}_{12}(r_1, r_2, t)$, and $P^{10}_{21}(r_1, r_2, t)$ radial wavefunctions used in the TDCC propagation of the ^{1}P excited state. The core orthogonalization expression found in equation (9) is similar to that used recently in the TDCC method for the electron-impact ionization of Li_2 [25].

For TDCC relaxation and propagation using a pseudopotential method, the radial mesh spacing Δr can be fairly sizeable. On the other hand, the radial mesh spacing Δr becomes much smaller to represent the inner closed subshell orbitals needed for the core orthogonalization method. Therefore, we make use of a variable radial mesh [26] which is continuously changing from a small Δr value near the origin to a larger Δr value at some distance outside the closed subshell orbitals, after which Δr remains constant.

Single and double photoionization probability functions are given by

$$\mathcal{P}_1(n_1 l_1, T) = \sum_{k_2, l_2} \left| \int dr_1 \int dr_2 P_{n_1 l_1}(r_1) P_{k_2 l_2}(r_2) \times P^{LS}_{l_1 l_2}(r_1, r_2, T) \right|^2 , \tag{10}$$

$$\mathcal{P}_2(n_2 l_2, T) = \sum_{k_1, l_1} \left| \int dr_1 \int dr_2 P_{k_1 l_1}(r_1) P_{n_2 l_2}(r_2) \times P^{LS}_{l_1 l_2}(r_1, r_2, T) \right|^2 , \tag{11}$$

$$\mathcal{P}(T) = \sum_{k_1, l_1} \sum_{k_2, l_2} \left| \int dr_1 \int dr_2 P_{k_1 l_1}(r_1) P_{k_2 l_2}(r_2) \times P^{LS}_{l_1 l_2}(r_1, r_2, T) \right|^2 , \tag{12}$$

and T is the final propagation time. The total cross section for single ionization is given by

$$\sigma_1(nl) = \frac{\omega}{I}\frac{\partial}{\partial T}[\mathcal{P}_1(nl, T) + \mathcal{P}_2(nl, T)] \tag{13}$$

and the total cross section for double ionization is given by

$$\sigma_2 = \frac{\omega}{I}\frac{\partial}{\partial T}\mathcal{P}(T) \, , \tag{14}$$

where ω is the radiation frequency and I is the radiation field intensity. The double to single photoionization ratio is given by

$$\mathcal{R} = \sigma_2 \Big/ \sum_{nl} \sigma_1(nl) \, . \tag{15}$$

3. Results

The TDCC method was first used to calculate photoionization cross sections for the Be atom. A variable mesh of 648 points with a starting value of $\Delta r = 0.01$ and a total radius of $R = 111.5$ was used in all of the calculations. Diagonalization of the one-electron Hamiltonian of equation (2) on the radial lattice yielded a complete set of bound and continuum radial orbitals needed to evaluate the photoionization probability functions of equations (10)–(12). Tuning of the α_l coefficient in equation (7) yielded binding energies for the 2s radial orbital of 18.2 eV and the 2p radial orbital of 14.2 eV, in agreement with Be^+ experimental values [27].

Relaxation of the TDCC equations in imaginary time, τ, on the 648 × 648 point lattice with 7 $l_1 l_2$ coupled channels was used to obtain the correlated initial state wavefunctions, $\bar{P}^{L_0 S}_{l_1 l_2}(r_1, r_2)$. We used an implicit propagator with $\Delta\tau = 0.025$. At each time step the $P^{00}_{00}(r_1, r_2, \tau)$ coupled channel was orthogonalized to the 1s orbital. The correlated initial state wavefunctions were found to have an energy $E_0 = -27.5$ eV, in agreement with the experimental double ionization potential of 27.5 eV for Be [27].

Propagation of the TDCC equations in real time, t, on the 648 × 648 point lattice with 12 $l_1 l_2$ coupled channels was used to obtain the correlated final state wavefunctions,

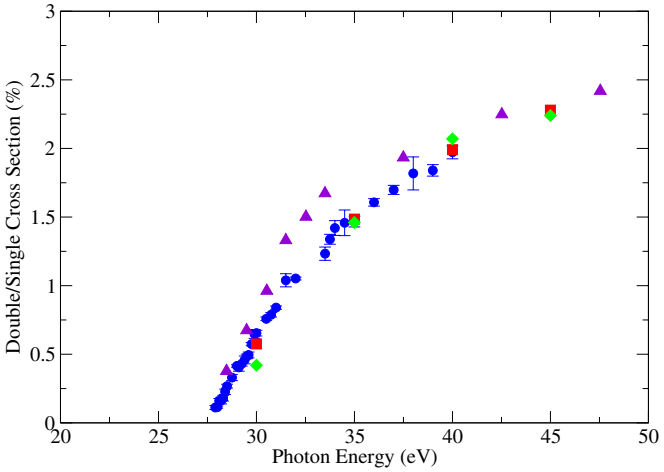

Figure 1. Double to single photoionization cross section ratio for the Be atom. Solid (red) squares: TDCC calculations, solid (violet) triangles: CCC calculations [17], solid (green) diamonds: RMPS calculations [14], solid (blue) circles with error bars: experiment [16].

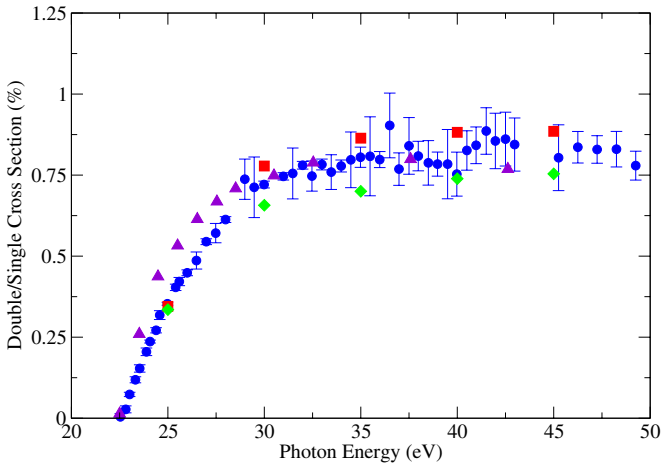

Figure 2. Double to single photoionization cross section ratio for the Mg atom. Solid (red) squares: TDCC calculations, solid (violet) triangles: CCC calculations [17], solid (green) diamonds: RMPS calculations [14], solid (blue) circles with error bars: experiment [18].

Table 1. Single photoionization cross sections for Be at an incident photon energy of 40 eV leaving Be^+ in the ground state (1.0 Kb = 1.0×10^{-21} cm^2).

RRPA [28]	MCTD [28]	CCC [17]	RMPS [14]	TDCC
630 Kb	440 Kb	545 Kb	490 Kb	528 Kb

$P^{LS}_{l_1 l_2}(r_1, r_2, t)$. We used an implicit propagator with $\Delta t = 0.01$. Calculations were made at photon energies of 30 eV, 35 eV, 40 eV, and 45 eV. At each time step the $P^{10}_{01}(r_1, r_2, t)$ and $P^{10}_{10}(r_1, r_2, t)$ coupled channels were orthogonalized to the 1s orbital. The photoionization probability functions of equations (10)–(12) were then calculated at a final time T corresponding to 15 radiation field periods.

The TDCC double to single photoionization cross section ratios, obtained using equations (13)–(15), are presented in figure 1 in comparison with CCC calculations [17], RMPS calculations [14], and experiment [16]. There is good overall agreement between theory and experiment. We note that no absolute experimental cross sections are currently available for the single or double photoionization of the Be atom. The TDCC absolute single photoionization cross section leaving Be^+ in the ground state, $\sigma(2s)$ of equation (13), is also found to be in reasonable agreement at a photon energy of 40 eV with calculations using the relativistic random phase approximation (RRPA) [28], the multi-configuration Tamm–Dancoff (MCTD) [28], the CCC [17], and the RMPS [14] methods, as presented in table 1.

The TDCC method was then used to calculate photoionization cross sections for the Mg atom. A variable mesh of 720 points with a starting value of $\Delta = 0.005$ and a total radius of $R = 105.9$ was used in all the calculations. Diagonalization of the one-electron Hamiltonian of equation (2) and tuning of the α_l coefficient in equation (7) yielded binding energies for the 3s radial orbital of 15.0 eV, the 3p radial orbital of 10.6 eV, and the 3d radial orbital of 6.2 eV, in agreement with Mg^+ experimental values [27].

Relaxation of the TDCC equations in imaginary time on the 720×720 point lattice with 7 $l_1 l_2$ coupled channels was used to obtain the correlated initial state wavefunctions. We used an implicit propagator with $\Delta\tau = 0.025$. At each time step the $P^{00}_{00}(r_1, r_2, \tau)$ coupled channel was orthogonalized to the 1s and 2s orbitals and the $P^{00}_{11}(r_1, r_2, \tau)$ coupled channel was orthogonalized to the 2p orbital. The correlated initial state wavefunctions were found to have an energy $E_0 = -22.8$ eV, in close agreement with the experimental double ionization potential of 22.7 eV for Mg [27].

Propagation of the TDCC equations in real time on the 720×720 point lattice with 12 $l_1 l_2$ coupled channels was used to obtain the correlated final state wavefunctions. We used an implicit propagator with $\Delta t = 0.01$. Calculations were made at 25, 30, 35, 40, and 45 eV. At each time step the $P^{10}_{01}(r_1, r_2, t)$ and $P^{10}_{10}(r_1, r_2, t)$ coupled channels were orthogonalized to the 1s, 2s, and 2p orbitals and the $P^{10}_{12}(r_1, r_2, t)$ and $P^{10}_{21}(r_1, r_2, t)$ coupled channels were orthogonalized to the 2p orbital. The photoionization probability functions of equations (10)–(12) were then calculated at a final time T corresponding to 15 radiation field periods.

The TDCC double to single photoionization cross section ratios, obtained using equations (13)–(15) are presented in figure 2 in comparison with CCC calculations [17], RMPS calculations [14], and experiment [18]. There is again good overall agreement between theory and experiment. We note that no absolute experimental cross sections are currently available for the single or double photoionization of the Mg atom. The TDCC absolute single photoionization cross section leaving Mg^+ in the ground state, $\sigma(3s)$ of equation (13), is also found to be in reasonable agreement at a photon energy of 30 eV with RRPA [28], MCTD [28], CCC [17], and RMPS [14] calculations, as presented in table 2. TDCC single photoionization cross sections leaving Mg^+ in the ground state at a photon energy of 30 eV are also presented in table 3. The cross section obtained using an implicit time propagator with a core orthogonalization method on a variable radial mesh is

Table 2. Single photoionization cross sections for Mg at an incident photon energy of 30 eV leaving Mg^+ in the ground state (1.0 Kb = 1.0×10^{-21} cm^2).

RRPA [28]	MCTD [28]	CCC [17]	RMPS [14]	TDCC
195 Kb	200 Kb	200 Kb	185 Kb	217 Kb

Table 3. Single photoionization cross sections for Mg at an incident photon energy of 30 eV leaving Mg^+ in the ground state (1.0 Kb = 1.0×10^{-21} cm^2).

TDCC method	Cross section
Implicit, core orthogonalization, variable mesh	217 Kb
Explicit, node removal pseudopotential, fixed mesh	105 Kb
Explicit, effective pseudopotential, fixed mesh	136 Kb

found to be considerably larger than the cross sections obtained using an explicit time propagator on a fixed $\Delta r = 0.10$ radial mesh with either an inner node removal pseudopotential method (see equation (8)) or an effective pseudopotential method [21].

4. Summary

In this paper, we have used a new version of the time-dependent close-coupling method (TDCC) to calculate the single and double photoionization of the Be and Mg atoms. An implicit time propagation of the close-coupling equations allows us to easily replace a core pseudopotential method on a coarse fixed radial mesh with a core orthogonalization method on a fine variable radial mesh. We find that the new version of the TDCC method yields double to single photoionization cross section ratios in good agreement with experiment for both Be and Mg. In the future, we plan to use the new version of the TDCC method to study a variety of photon, electron, and heavy particle collisions with atoms and their ions. For example, atomic collision processes that involve the ejection of an inner subshell electron need a fine radial mesh for which the implicit time propagator is ideal.

Acknowledgments

We would like to thank Professor Ralf Wehlitz of the University of Wisconsin for providing us with experimental data files for both Be and Mg. This work was supported in part by grants from the US Department of Energy and the US National Science Foundation. Computational work was carried out at the National Energy Research Scientific Computing Center in Oakland, California, and the National Institute for Computational Sciences in Knoxville, TN.

References

[1] Leven J C, Armen G B and Sellin I A 1996 *Phys. Rev. Lett.* **76** 1220
[2] Dorner R *et al* 1998 *Phys. Rev.* A **57** 1074
[3] Marchalant P J and Bartschat K 1997 *Phys. Rev.* A **56** R1697
[4] Gorczyca T W and Badnell N R 1997 *J. Phys. B: At. Mol. Opt. Phys.* **30** 3897
[5] Selles P, Malegat L and Kazansky A K 2002 *Phys. Rev.* A **65** 032711
[6] Feng L and van der Hart H W 2002 *Phys. Rev.* A **66** 031402
[7] Scott M P, Kinnen A J and McIntyre M W 2012 *Phys. Rev.* A **86** 032707
[8] Kheifets A S and Bray I 1998 *J. Phys. B: At. Mol. Opt. Phys.* **31** L447
[9] Colgan J, Pindzola M S and Robicheaux F 2001 *J. Phys. B: At. Mol. Opt. Phys.* **34** L457
[10] McCurdy C W, Horner D A, Rescigno T N and Martin F 2004 *Phys. Rev.* A **69** 032707
[11] Kheifets A S and Bray I 2002 *Phys. Rev.* A **65** 012710
[12] Colgan J and Pindzola M S 2002 *Phys. Rev.* A **65** 022709
[13] Citrini F, Malegat L, Selles P and Kazansky A K 2003 *Phys. Rev.* A **67** 042709
[14] Griffin D C, Pindzola M S, Ballance C P and Colgan J 2009 *Phys. Rev.* A **79** 023413
[15] Lukic D, Bluett J B and Wehlitz R 2004 *Phys. Rev. Lett.* **93** 023003
[16] Wehlitz R, Lukic D and Bluett J B 2005 *Phys. Rev.* A **71** 012707
[17] Kheifets A S and Bray I 2007 *Phys. Rev.* A **75** 042703
[18] Wehlitz R, Juranic P N and Lukic D V 2008 *Phys. Rev.* A **78** 033428
[19] Malegat L, Citrini F, Selles P and Archirel P 2000 *J. Phys. B: At. Mol. Opt. Phys.* **33** 2409
[20] Yip F L, McCurdy C W and Rescigno T N 2010 *Phys. Rev.* A **81** 053407
[21] Wadt W R and Hay P J 1985 *J. Chem. Phys.* **82** 284
[22] Pindzola M S *et al* 2007 *J. Phys. B: At. Mol. Opt. Phys.* **40** R39
[23] Pindzola M S, Robicheaux F and Colgan J 2005 *J. Phys. B: At. Mol. Opt. Phys.* **38** L285
[24] Froese Fischer C 1987 *Comput. Phys. Commun.* **43** 355
[25] Pindzola M S, Abdel-Naby Sh A, Ludlow J A, Robicheaux F and Colgan J 2012 *Phys. Rev.* A **85** 012704
[26] Witthoeft M C, Pindzola M S and Colgan J 2003 *Phys. Rev.* A **67** 032713
[27] http://physics.nist.gov/PhysRefData
[28] Radojevic V and Johnson W R 1985 *Phys. Rev.* A **31** 2991